Global Change and the Dark of the Moon

S. Flatté
S. Koonin
G. MacDonald

ADA255 181

June 1992

JSR-91-315

Distribution unlimited; open for public release.

JASON
The MITRE Corporation
7525 Colshire Drive
McLean, Virginia 22102-3481
(703) 883-6997

REPORT DOCUMENTATION PAGE

Form Approved
OMB No. 0704-0188

1. AGENCY USE ONLY *(Leave blank)*

2. REPORT DATE
June 30, 1992

3. REPORT TYPE AND DATES COVERED
Final

4. TITLE AND SUBTITLE
Global Change and the Dark of the Moon

5. FUNDING NUMBERS
PR - 8503Z

6. AUTHOR(S)
S. Flatte', S. Koonin, G. MacDonald

7. PERFORMING ORGANIZATION NAME(S) AND ADDRESS(ES)
The MITRE Corporation
JASON Program Office A10
7525 Colshire Drive
McLean, VA 22102

8. PERFORMING ORGANIZATION REPORT NUMBER
JSR-91-315

9. SPONSORING/MONITORING AGENCY NAME(S) AND ADDRESS(ES)
Department of Energy
Office of Program Analysis
Office of Energy Research
Washington, DC 20585

10. SPONSORING/MONITORING AGENCY REPORT NUMBER
JSR-91-315

11. SUPPLEMENTARY NOTES

12a. DISTRIBUTION/AVAILABILITY STATEMENT
Distribution unlimited; open for public release.

12b. DISTRIBUTION CODE

13. ABSTRACT *(Maximum 200 words)*

We have considered the possibility of using earthshine to measure the reflectance properties of the earth (albedo and phase function). Measurements of earthshine carried out by Danjon in 1926--33 show that even then the average albedo could be determined with a precision of $\pm$ 0.01 and that both synoptic and seasonal variations could be observed clearly.

We show that, after correction for wavelength dependence and the opposition effect in the lunar reflectance properties, Danjon's visual albedo of 0.40 can be reconciled with the ERBE satellite Bond albedo of 0.30. We recommend a modern earthshine monitoring program (advantages include global integration, continuous coverage, ground basing, and low cost) as a complement to present and planned satellite measurements.

14. SUBJECT TERMS
earth albedo, earthshine, elementary photometry, danjon's measurements

15. NUMBER OF PAGES

16. PRICE CODE

17. SECURITY CLASSIFICATION OF REPORT	18. SECURITY CLASSIFICATION OF THIS PAGE	19. SECURITY CLASSIFICATION OF ABSTRACT	20. LIMITATION OF ABSTRACT
UNCLASSIFIED	UNCLASSIFIED	UNCLASSIFIED	SAR

Contents

1 EXECUTIVE SUMMARY

We have considered the possibility of using earthshine to measure the reflectance properties of the earth (albedo and phase function). Measurements of earthshine carried out by Danjon in 1926–33 show that even then the average albedo could be determined with a precision of ± 0.01 and that both synoptic and seasonal variations could be observed clearly.

We show that, after correction for wavelength dependence and the opposition effect in the lunar reflectance properties, Danjon's visual albedo of 0.40 can be reconciled with the ERBE satellite Bond albedo of 0.30. We recommend a modern earthshine monitoring program (advantages include global integration, continuous coverage, ground basing, and low cost) as a complement to present and planned satellite measurements.

2 INTRODUCTION

In this report we consider a "new" monitor of global change: observations of earthshine as a measure of the earth's albedo and phase function. This is actually the oldest method of determining the earth's albedo [1], and was studied extensively from 1926–33 by Danjon [2, 3]. Very little has been done since [4], we suspect in part because of lack of intense interest in the subject and because of the advent of satellite measurements. However, earthshine has several clear advantages in a modern context, as we hope to demonstrate.

We begin our presentation with a brief discussion of the importance of the earth's albedo to climate. We then turn to a qualitative discussion of earthshine and review the relevant notions of photometry. This is followed by a review of Danjon's measurements, both to illustrate the method and to show what could be done even with 1920s technology. We note several corrections to Danjon's observations and show how they can be reconciled with satellite measurements. Finally, we discuss some possibilities for modern earthshine measurements.

3 THE EARTH'S ALBEDO AND ITS CLIMATE

The earth's climate system is basically a large heat engine. Energy comes into the system in the form of short-wavelength radiation from the sun, peaking at a wavelength of 0.5μm (a black-body temperature of about 6000 K) (see Figure 1). Almost 99 percent of the sun's radiation is contained in the so-called short wavelength region of 0.15 to 4.0 μm. Of this energy 46 percent is in the infrared region above 0.74 μm, 9 percent in the ultraviolet below 0.4 μm and the remaining 45 percent in the visible, 0.4 to 0.74 μm. A significant fraction of this energy is absorbed by the earth, where it drives the motion of the atmosphere and oceans before being radiated back into space as long-wavelength radiation peaking at a wavelength of 15 μm (a black-body temperature of $T_E = 255$ K).

The power going in to the earth's climate system is

$$P_{in} = C\pi R_E^2(1 - A) \, , \tag{3-1}$$

where $C = 1370$ W/m^2 is the solar constant, $R_E = 6378$ km is the earth's radius, and $A = 0.30$ is the earth's shortwave (Bond) albedo, giving the fraction of the incident shortwave solar radiation (between 0.15 and 4.0 μm) that is reflected from the earth without being absorbed. For this latter quantity, we have adopted the value determined by ERBE satellite measurements [6]. Similarly, the longwave power that the planet radiates into space is

$$P_{out} = 4\pi R_E^2 \sigma \epsilon T_E^4 \, , \tag{3-2}$$

where σ is the Stefan-Boltzmann constant and ϵ is the emissivity at the top of the atmosphere (about 5.5 km, where the long wave radiation is emitted).

If the planet is in radiative equilibrium, these two powers are equal,

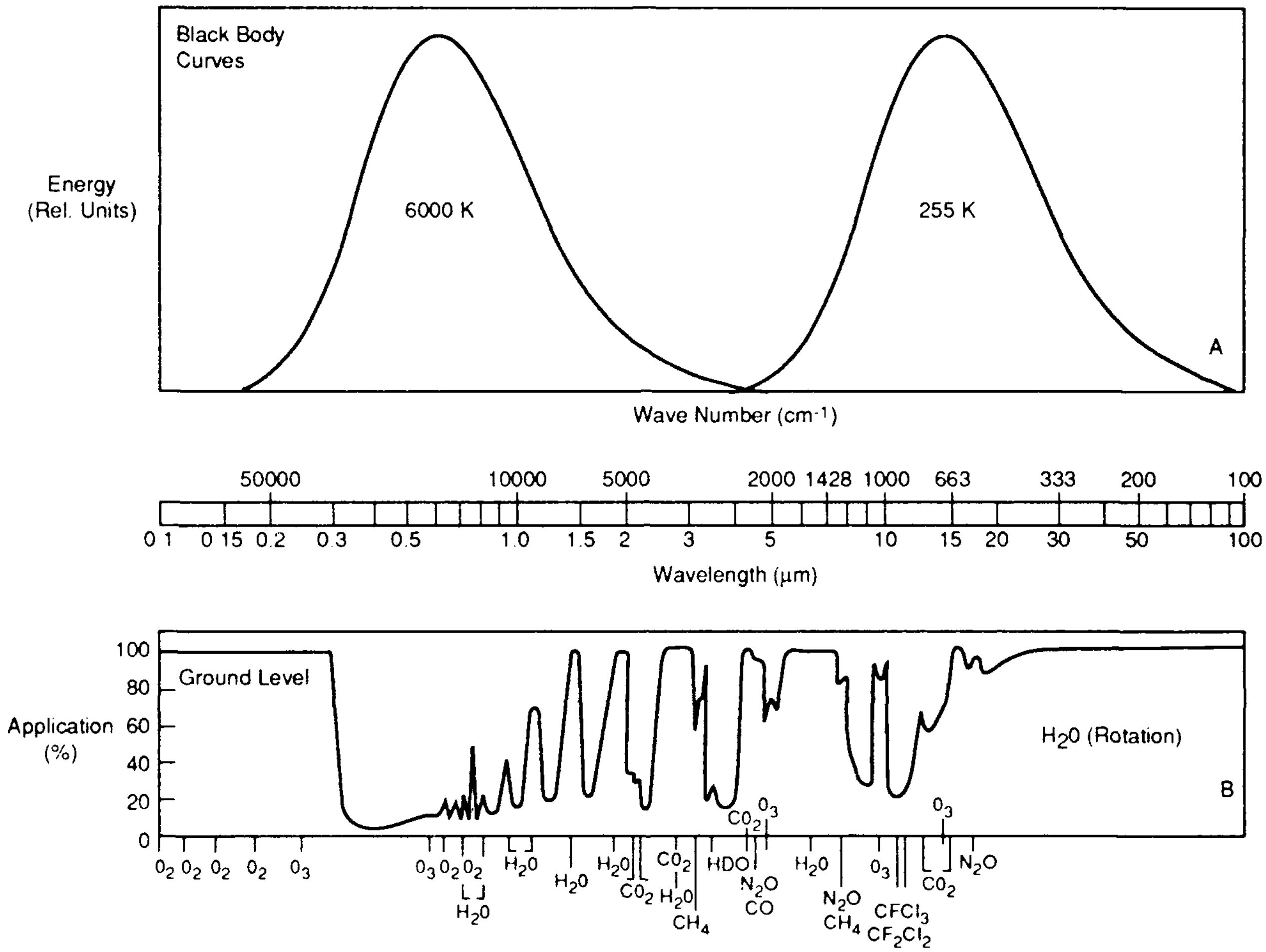

Figure 1. (A) Spectral distribution of longwave emission from black bodies at 6000 K and 255 K, corresponding to the mean emitting temperatures of the sun and earth, respectively, and (B) percentage of atmospheric absorption for radiation passing from the top of the atmosphere to the surface. Notice the comparatively weak absorption of the solar spectrum and the region of weak absorption from 8 to 12 μm in the longwave spectrum (from Reference [5]).

giving

$$T_E^4 = \frac{C}{4\sigma\epsilon}(1 - A)\ . \qquad (3\text{–}3)$$

Thus, the global shortwave albedo directly controls the earth's temperature.

Most (about 70 percent) of the solar energy entering the climate system is absorbed by the surface or within the atmosphere, with the balance being reflected. The energy budgets of the three principal kinds of surfaces that cover the earth differ dramatically. The heat capacity of the oceans is very large and the solar radiant energy can penetrate efficiently. The oceans thus respond slowly to changes in solar flux and act as the regulators of the climate system. Snow and ice reflect a large fraction of the incoming radiation (albedo up to 0.8). The albedo does not change until near the melting point, when the optical character of the surface begins to alter. Because of the phase change, snow and ice have a large effective heat capacity and influence primarily the slow physics of the atmosphere. Land surfaces respond most rapidly to changes in solar radiation. Their effective heat capacity is low because visible light does not penetrate and thermal conduction is very slow. The albedo of the land surface depends on the angle of the incident radiation and, when the land is covered with vegetation, on the spectrum of the incident radiation.

The global albedo depends upon the reflectance properties of each surface element of the earth. Any good quality radiation detector (e.g., pyranometer) can be used to measure albedo. Two instruments, one looking upward and the other downward, will provide an instantaneous measure of downwelling and upwelling radiation. The instruments may be at ground level or on an aircraft or satellite, depending on the area to be viewed.

The value obtained by an instrument will depend on the zenith angle of the sun, the transmittance of the atmosphere, the nature of the surface, and the nature of the cloud cover, if any, including the thickness of the cloud, the water content of the cloud, and the droplet size distribution within the cloud. The angle of the reflecting surface to the horizontal, particularly if it is facing towards or away from the sun, is important. The surface albedo is high for dry, light-colored, smooth surfaces and is low for wet, dark-colored, rough surfaces. In the case of vegetation the surface albedo will depend on the height of plants, percentage of ground cover, angle of leaves and the leaf area index. Figure 2 shows that, on average, the air and land each contribute about 25 percent of the reflectivity, with clouds making up the other 50 percent.

Typical albedos for clear land and ocean are 0.16 and 0.08, respectively, while the corresponding overcast values are 0.50 and 0.44; the albedo for clear desert is 0.23, while that for snow is 0.68. Local albedos show considerable synoptic and diurnal variability (see Figure 3). The global albedo also shows a seasonal variability, in part because of the greater land area in the Northern Hemisphere (see Figure 4).

Although it is the (effective) top-of-the-atmosphere temperature that appears in Equation (3-3), the surface temperature should also vary with albedo. This is borne out by the data presented in Figure 5, where the monthly mean global surface temperatures are plotted against the monthly mean global albedo for 100 years of an atmospheric general circulation model (GCM) run with the sea surface temperatures having a fixed seasonal cycle [7]. Perhaps coincidentally, the linearization of Equation (3-3) ($\Delta A/\Delta T_E = -0.01\ \mathrm{K}^{-1}$) is a reasonable description of the data. A similar conclusion can be drawn from the observations shown in Figure 6, where the monthly mean global temperatures for 1985 are plotted against the monthly mean global albedos determined by ERBE [6].

Greenhouse warming scenarios give ambiguous predictions of the likely change in the albedo. On the one hand, the increasing water vapor in the atmosphere could increase the cloudiness and hence the albedo. However,

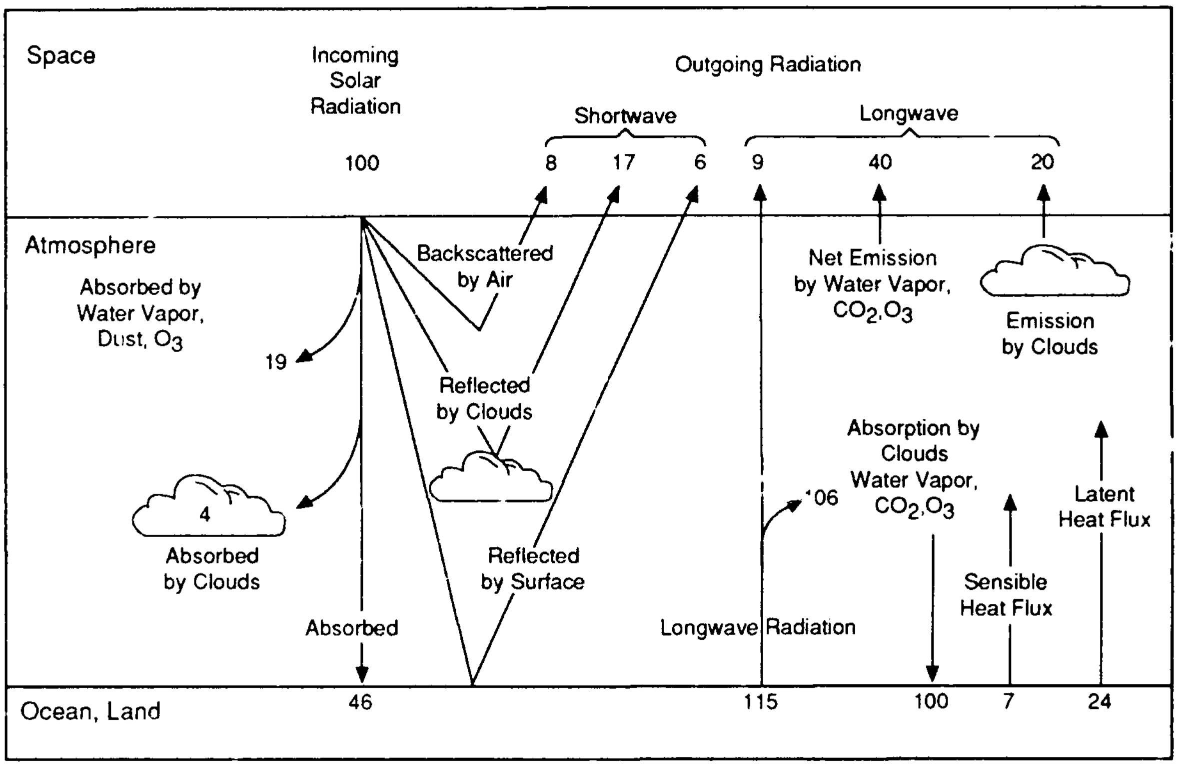

Figure 2. Schematic representation of the atmospheric heat balance. The units are percent of incoming solar radiation. The solar fluxes are shown on the left-hand side, and the longwave (thermal IR) fluxes are on the right-hand side (from Reference [5]).

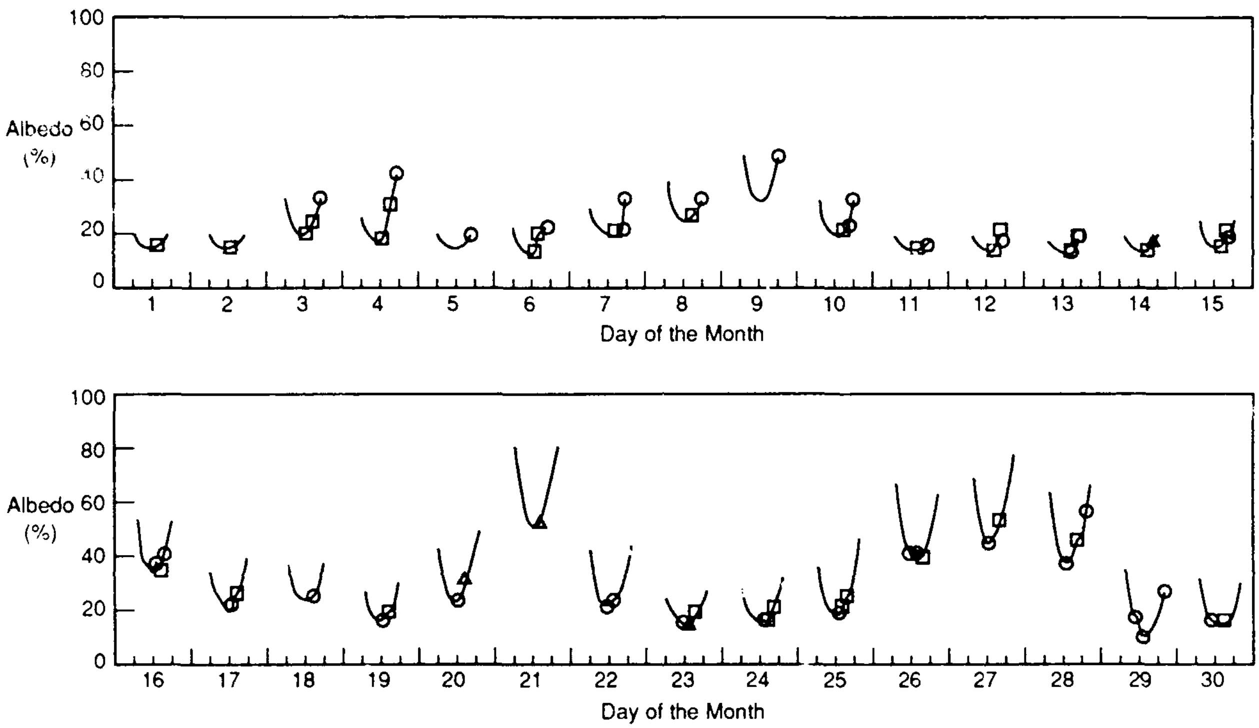

Figure 3. Time history of April 1985 albedo for a region in the western Pacific Ocean (long. = 148.75°W, lat. = 21.25°S) (from Reference [6]).

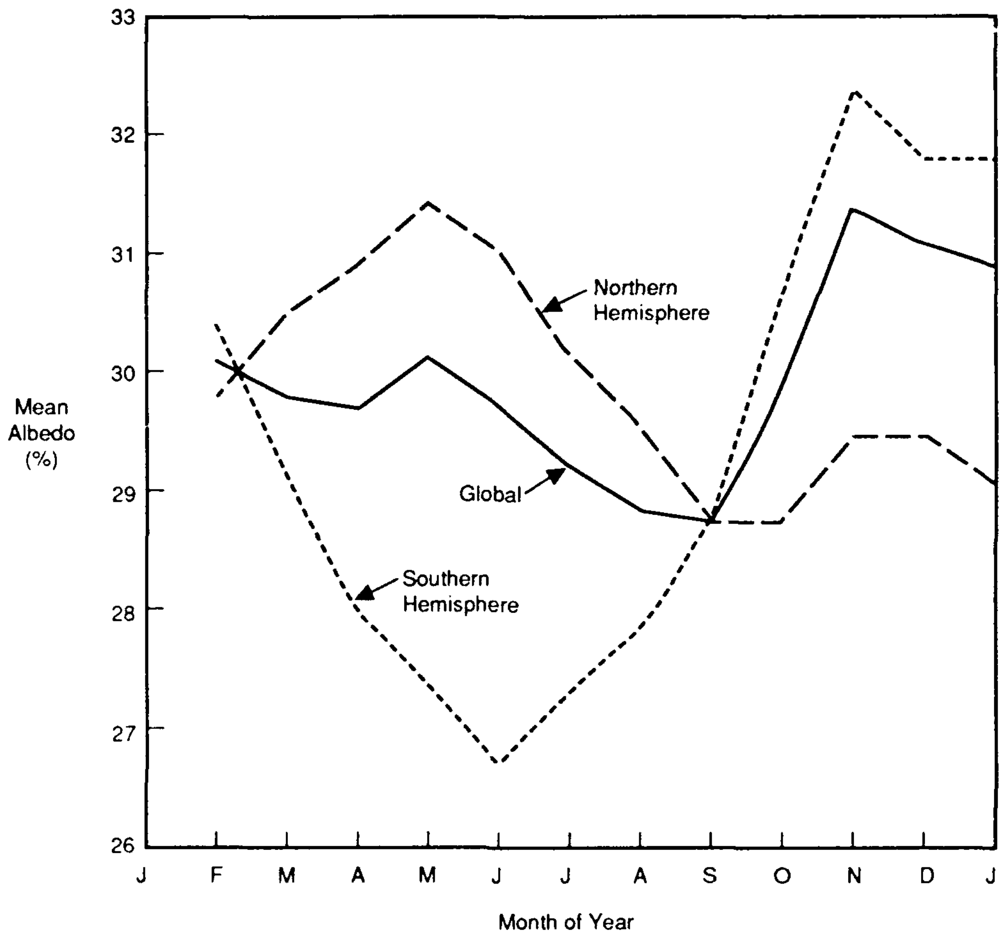

Figure 4. Annual variation of ERBE monthly mean albedo for hemispheres and the globe (from Reference [6]).

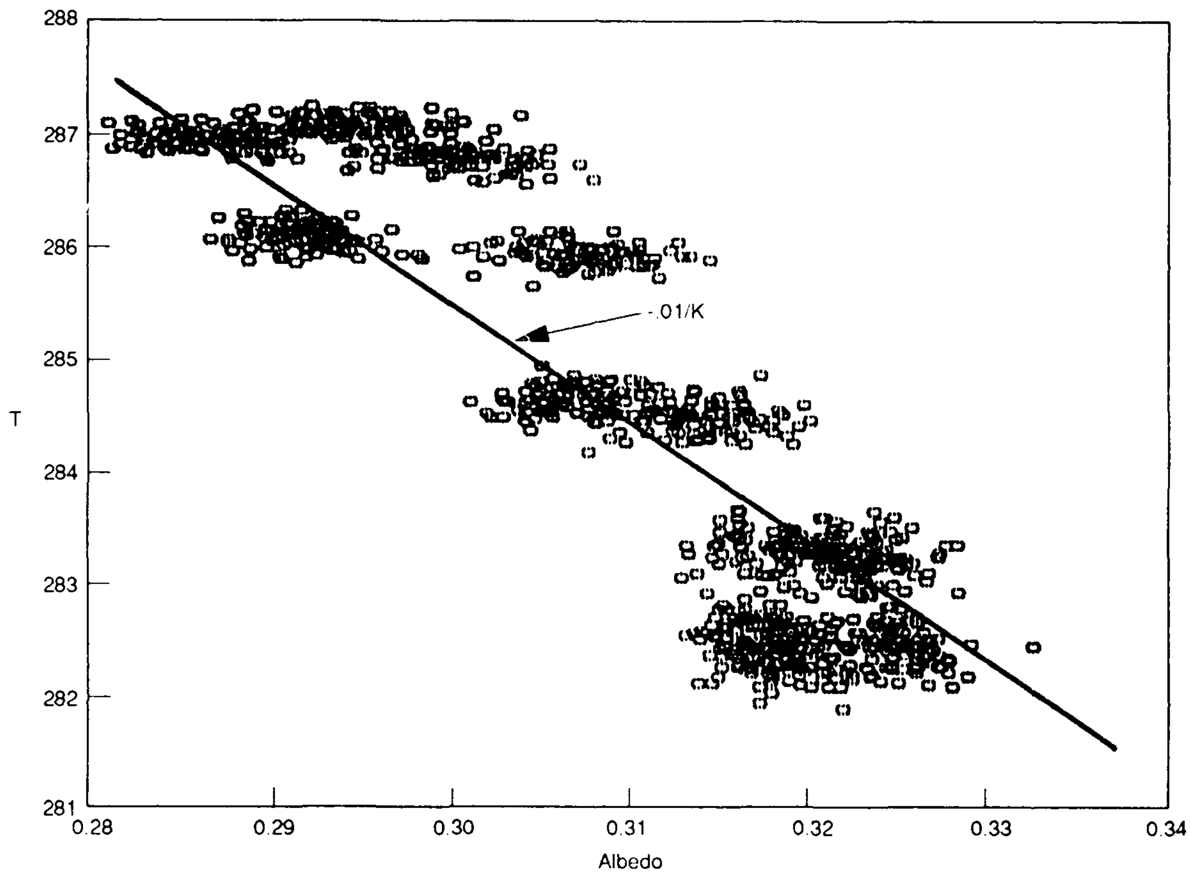

Figure 5. Correlation of the monthly mean globally averaged surface temperature with the monthly mean global albedo in a 100-year run of the NCAR CCM-1 with climatological sea-surface temperatures (from Reference [7]).

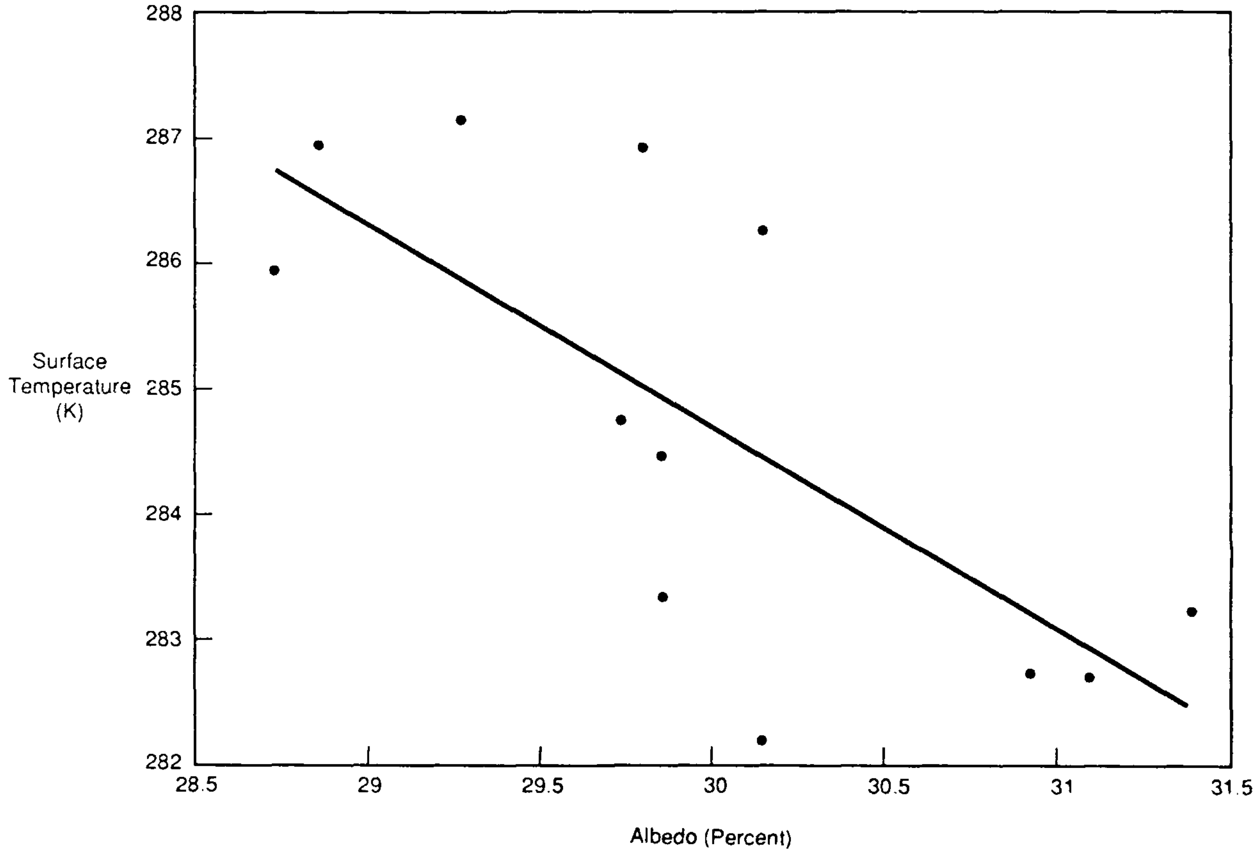

Figure 6. Correlation of the monthly mean global surface temperature with the ERBE monthly mean albedo for 1985. The least-squares fit line shown has a slope of -0.016/K.

the decreasing snow and ice coverage will act to decrease the albedo. The net effect need not be negative (as might be expected from Equation (3-3) as the temperature increases), as the emissivity of the atmosphere will change with increasing greenhouse gas content.

The most precise measurements of the earth's albedo come from satellite measurements such as those of ERBE [6, 8]. Here an instrument measures the amount of outgoing shortwave radiation for one spot on the earth at one particular solar zenith angle from a given viewing elevation and azimuth. Complex "scene" models are then used to convert this measurement into a total flux of outgoing shortwave radiation (i.e., that going into all viewing directions) and hence an albedo; further modeling is used to average over the diurnal cycle (zenith angle dependence). Finally, all pixel values are averaged to obtain a global value. The process is quite complex, with many modeling assumptions involved. Other drawbacks of such measurements include the expense and risk of satellites and the difficulty of maintaining a very accurate calibration (better than 1 percent) in a space-based instrument. Although great effort has been expended to ensure the accuracy of satellite-determined albedos, an independent check would be, at the least, reassuring.

4 EARTHSHINE

Earthshine is sunlight that is reflected by the earth to the moon (see Figure 7). It therefore contributes to the illumination of the moon beyond that of the much more intense direct sunshine and is most easily visible as a ghostly glow of the dark portion of the lunar disk. The phenomenon was known to the ancients and understood by Kepler in 1604.

The geometry of the sun-earth-moon system is most simply characterized by the sun-moon-earth angle ψ, the phase angle of the moon (see Figure 8). Because the earth-moon distance is much smaller than the earth-sun distance (ratio $\approx 2.5 \times 10^{-3}$), the sun-earth-moon angle, or phase angle of the earth, is $\phi \approx \pi - \psi$. It is clear that earthshine will be most easily visible when ψ is largest (crescent moon as seen on earth and full earth as seen on the moon), although groundbased measurements for the very largest ψ are precluded by daylight. Conversely, earthshine is most difficult to observe when the moon is nearly full and the earth is a crescent ($\psi \approx 0$).

The use of a coronagraph enables observation of the earthshine as close as 38 hours before full moon [9], even though at this time the earthshine comes from a very narrow crescent of the earth and scattering and diffraction effects are relatively strong. The ratio of earthshine to sunshine visible from the earth thus varies throughout the lunar cycle; it is less than about 10^{-3} under the most favorable conditions.

To first order, earthshine observations measure scattered light in the plane of the ecliptic. The assumption of incident azimuth independence makes the observations general. The relations between the longitudes of the sun, the moon, and the observation station are described in Figures 9 and 10.

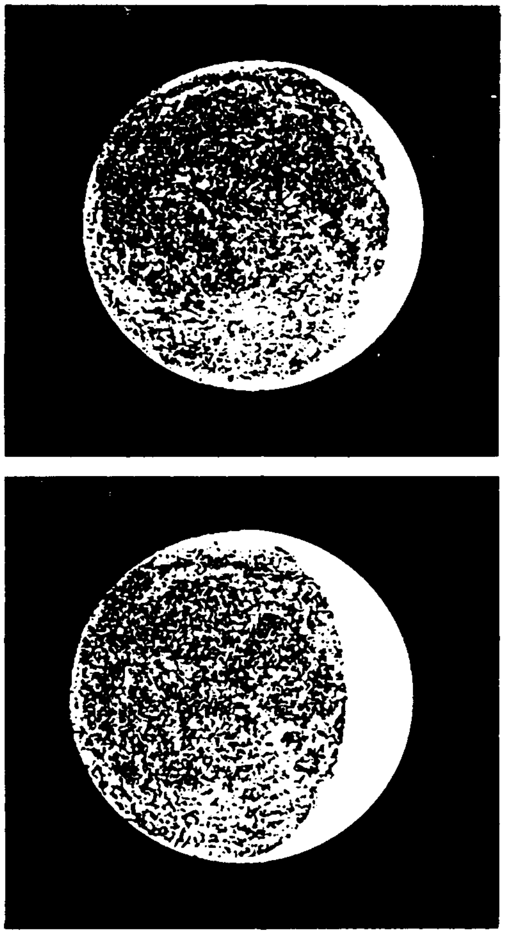

Figure 7. Photographs of the earthshine at various lunar phases (from Reference [2]).

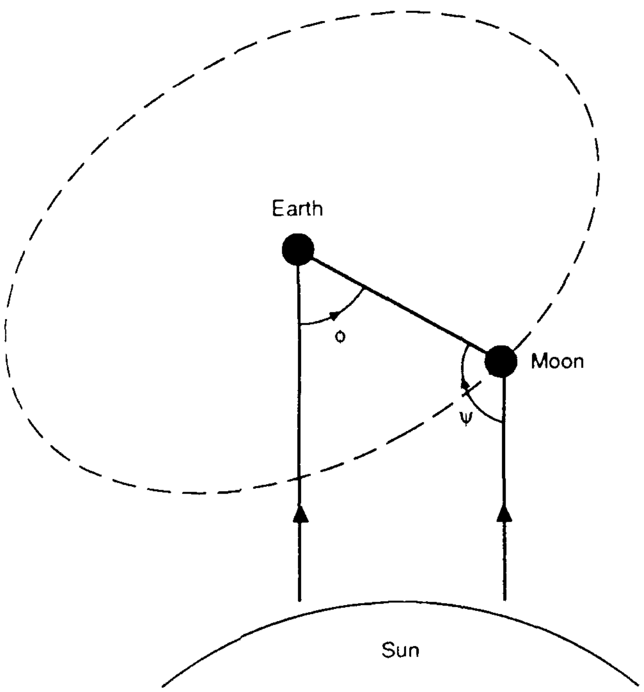

Figure 8. Geometry of the earth-moon-sun system. The earth's phase angle Φ is related to the moon's phase angle Ψ as $\Phi \approx \pi - \Psi$.

Earthshine clearly depends upon the visible reflectance properties of the earth and thus can be used to determine the earth's albedo. Such measurements were pursued by Very in 1912 [1] and more extensively by Danjon [2]. In a modern context they offer a number of attractive advantages, including an instantaneous coverage of a large region of the globe, the potential for nearly continuous long time series of observations, and the fact that they are ground based (and are hence relatively inexpensive and easily maintained, calibrated, and upgraded).

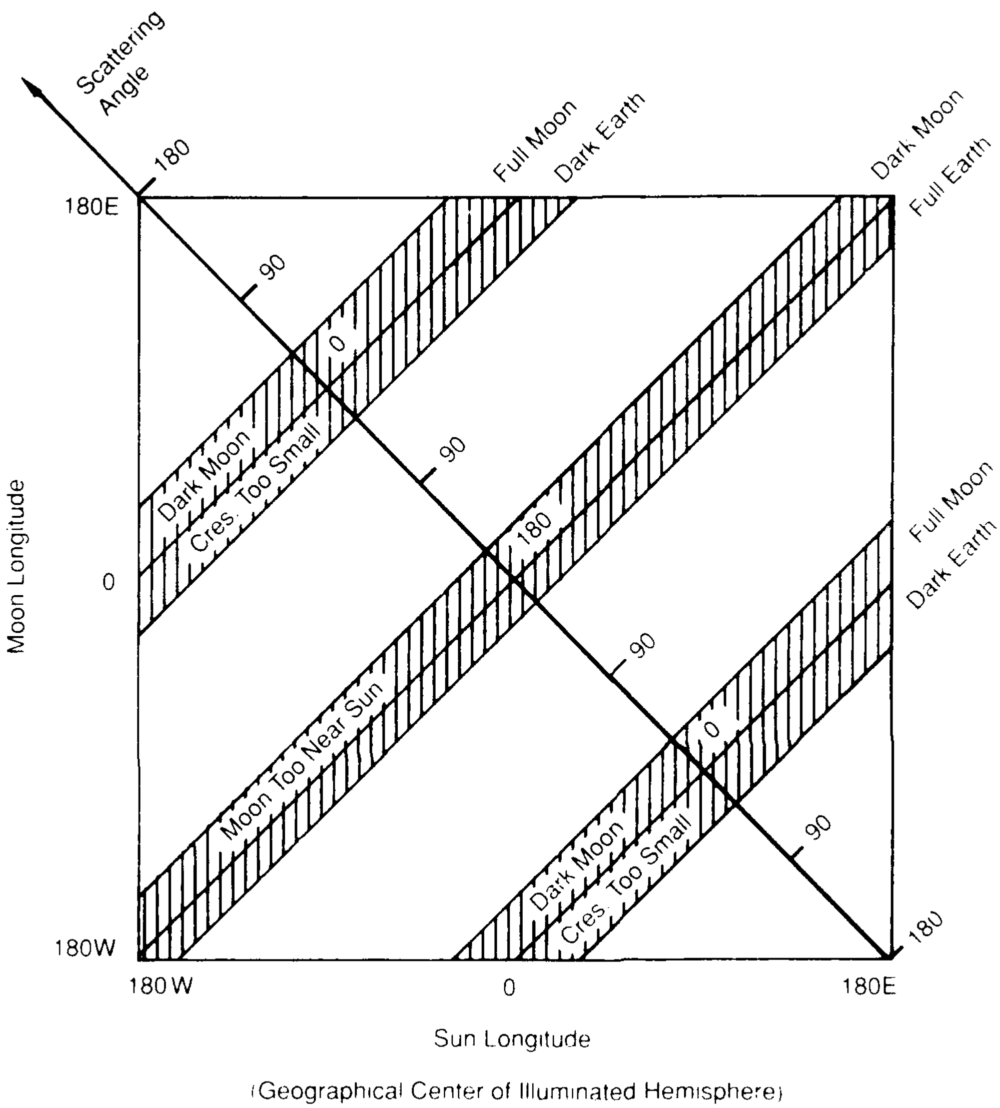

Figure 9. Geometrical relationships involved in earthshine measurements. The tilt of the earth's axis has been ignored. The earth's albedo is a function of the Sun longitude (which part of the earth is being illuminated) and time. The albedo is proportional to the integral of the scattered light over all directions; earthshine observations give measurements of the angular distribution in the plane of the ecliptic. The angle of scattering is indicated along the diagonal. Measurements are difficult or impossible too near either a full moon or a new moon, indicated by hatched areas.

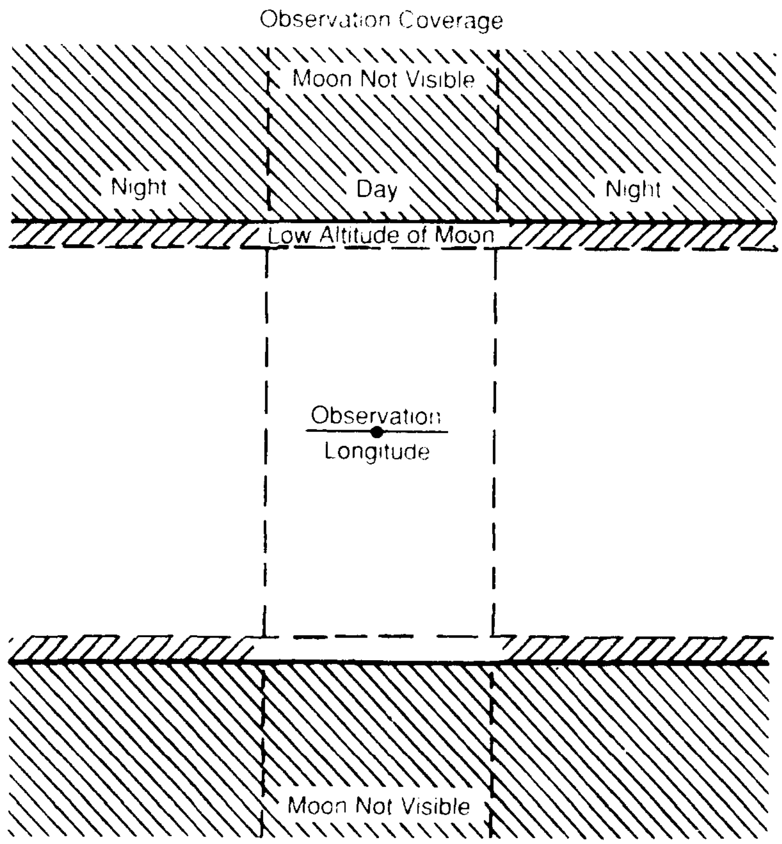

Figure 10. Coverage of the Sun/Moon Longitude diagram (Figure 9) possible from a given observation point near the equator. Figure 10 is meant to be overlaid on Figure 9 with the Observation Longitude point in the middle of Figure 10 placed on the positive diagonal of Figure 9 at the point where both the Sun and the Moon longitudes are equal to the chosen Observation Longitude. Then earthshine observations are possible in the clear areas; in the hatched areas of Figure 10 the moon is either below the horizon (and hence not visible) or is so close to the horizon that the earth's atmosphere interferes with the measurements. The regions of day or of night are indicated; some measurement systems (but not all) will be usable in the daytime.

5 ELEMENTARY PHOTOMETRY

In order to describe the use of earthshine to determine the earth's albedo, it is necessary to review some elementary notions of photometry. Consider, as shown in Figure 11, a plane surface of area S illuminated uniformly by light making an angle θ_i with the normal and observed at a similarly defined angle θ_r and azimuth χ_r. In general, the cross section for the plane to effect this scattering will depend upon all three angles, plus the azimuth of the incoming light. Dependence on the latter is usually ignored.

However, for a perfectly diffuse scatter (Lambert surface), the cross section is given by the azimuth-independent expression

$$\frac{d\sigma}{d\Omega_r} = Sr\frac{1}{\pi}\cos\theta_i\cos\theta_r \ , \qquad (5-1)$$

where Ω_r is the solid angle of scattering and r is the reflectance of the surface material. As expected, the total cross section for scattering is $\int d\Omega_r(d\sigma/d\Omega_r) = Sr\cos\theta_i$, the product of the reflectance and the projection of the illuminated area on the direction of illumination. We also note that when $\theta_r = \theta_i$, $d\sigma/d\Omega_r = (Sr/\pi)\cos^2\theta_i$.

Now consider the more complex situation of the earth illuminated by the sun. For a given phase angle ϕ, the cross section for light scattering can be written as

$$\frac{d\sigma}{d\Omega} = \pi R_E{}^2\frac{1}{\pi}pf_E(\phi) \ . \qquad (5-2)$$

Here, the earth's phase function f_E is defined so that $f_E(0) = 1$, implying that the cross section for the earth to backscatter the sunlight (and hence the intensity of the full earth) is given by $pR_E{}^2$. The quantity p is called the geometric albedo and depends upon the reflectance properties of

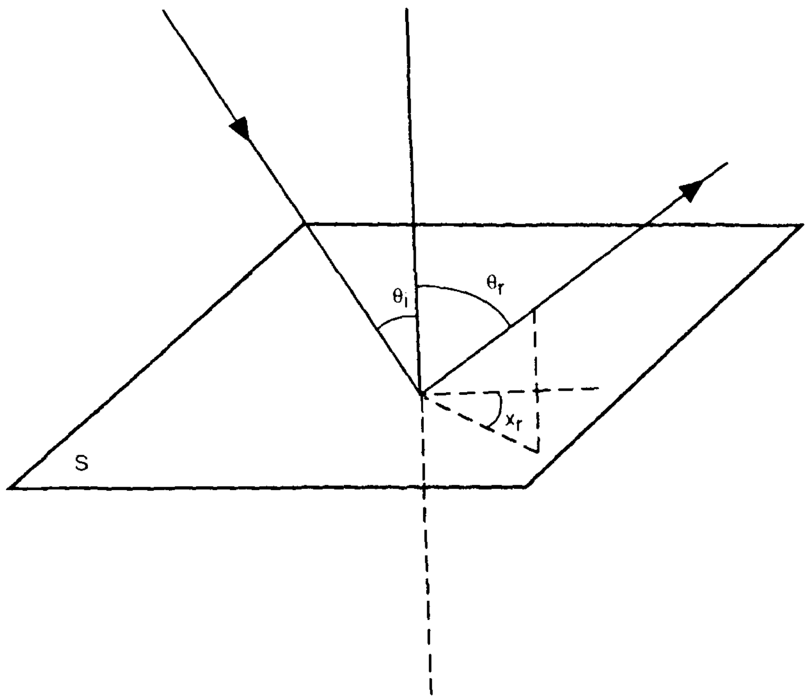

Figure 11. A plane reflector of area S illuminated at an angle θ_i and observed at angle θ_r with azimuth x_r.

the earth's surface and the geometry of a sphere. From its definition, it can be seen that p is the ratio of the light backscattered by the sphere to that backscattered by a normally illuminated perfectly reflecting ($r = 1$) Lambert disk of the same area (πR_E^2). For a Lambert sphere, $p = 2r/3$ and $f(\phi) = (\sin\phi + (\pi - \phi)\cos\phi)/\pi$. It should be noted that since the earth has a variegated surface, both p and f_E will depend upon the particular hemisphere illuminated.

The Bond albedo is, by definition, the ratio of the total cross section to the area of the planet's disk (πR_E^2). Thus,

$$A = pq\ ; \qquad q = \int_{-\pi}^{\pi} f_E(\phi)\sin\phi d\phi\ . \tag{5-3}$$

where q is termed the phase integral. A basic difficulty in albedo measurements is thus apparent: any one observation of the reflected light (whether a given view from a satellite or the earthshine at a given phase of the moon) determines the cross section at only one scattering angle, so that some extrapolation to all scattering angles must be performed to obtain the entire phase function and hence the phase integral. In satellite measurements, this is done by scene models; for the earthshine, it is done partially by measuring f_E at various phases. More generally, for earthshine it is necessary to make assumptions about (or models for) the sunlight scattered out of the ecliptic.

Many decades of photometry have determined the phase function, geometric albedo, phase integral, and visual albedo for various solar system objects. For example, the phase function of the moon as determined by Rougier [10] is shown in Figure 12, taken from [11].

Selected values of the phase integral and albedo are: Mercury (0.563,0.055), Venus (1.296,0.61), earth (1.095,0.40), and the moon (0.584,0.073), as given by Danjon [3].

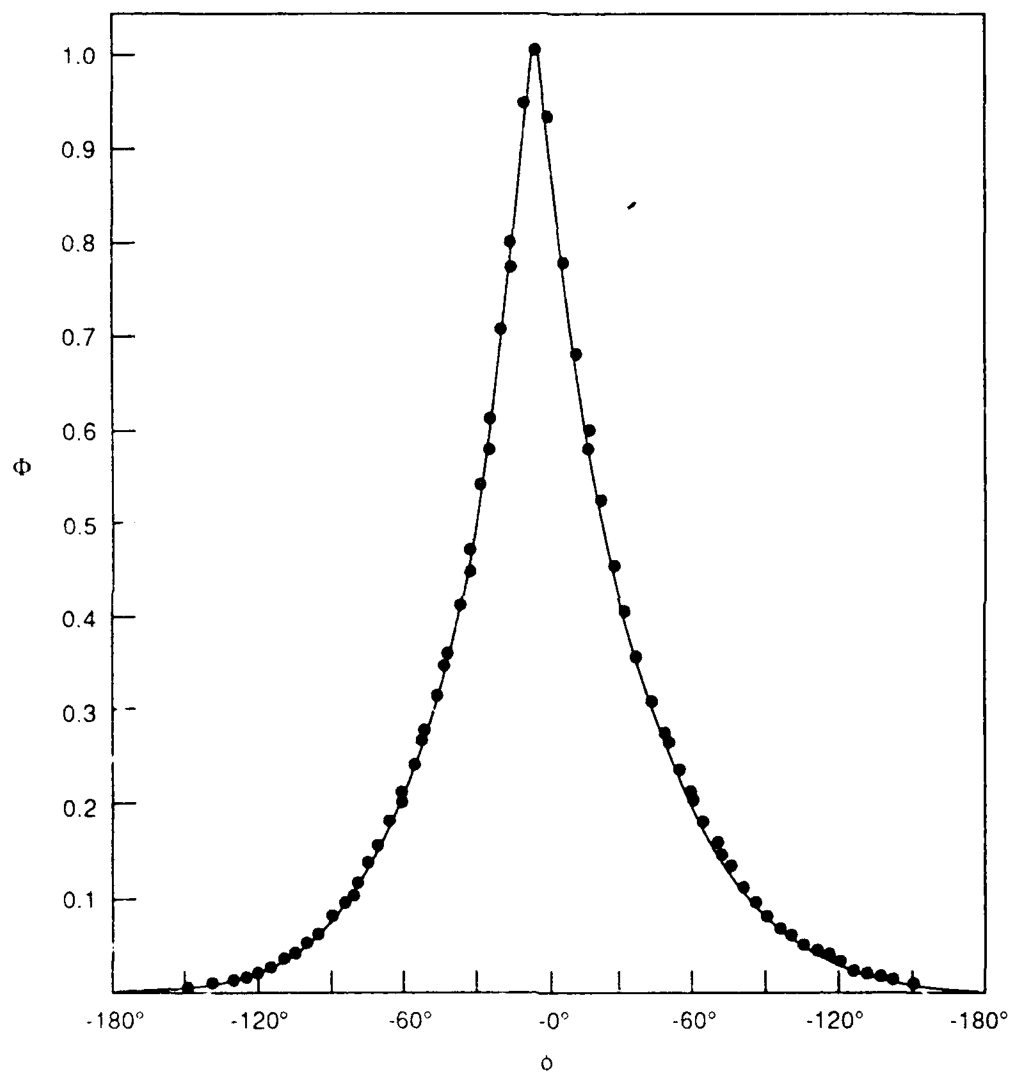

Figure 12. Integral phase function of the moon (from Reference[10]).

6 DANJON'S MEASUREMENTS

Danjon's measurements of earthshine [2, 3] involved comparing the intensities of two well defined patches of the lunar surface (denoted by A and B), with one in the sunshine and the other in the earthshine. The patches were chosen to be bright (highland) with similar optical properties and almost diametrically opposite near the lunar limb (see Figure 13). A photometer produced adjacent images of the moon, so that patch A in the earthshine was adjacent to patch B in the sunshine (see Figure 14). An adjustable diaphragm ("cat's eye") reduced the intensity of the light from B to allow the ratio of the intensities, $D_{AB} = I_A/I_B$, to be measured for various phase angles. For opposite phase, the roles of the patches were reversed.

Such differential measurements removed many of the uncertainties associated with atmospheric absorption, varying solar constant, etc.

Since the earthshine is backscattered from patch A while the sunshine scatters from B with phase angle ψ, the observed ratio of the intensities is

$$D_{AB} = \frac{I_E \frac{1}{\pi} p_A f_A(0)}{I_S \frac{1}{\pi} p_B f_B(\psi)} = \frac{I_E}{I_S} \frac{1}{f_M(\psi)} \tag{6-1}$$

where I_E and I_S are the intensities of the earth and sun as observed on the moon, $p_{(A,B)}$ are the geometric albedos, and $f_{(A,B)}$ are the phase functions. The second equality follows from assuming that $p_A = p_B$ and that $f_A = f_B = f_M$, a common phase function for both lunar patches. Note that if these assumptions were not valid, there would be systematic differences between observations during the positive and negative phases of the moon.

Solving Equation (6-1) for the ratio of intensities yields

$$\frac{I_E}{I_S} = D_{AB} f_M(\psi) . \tag{6-2}$$

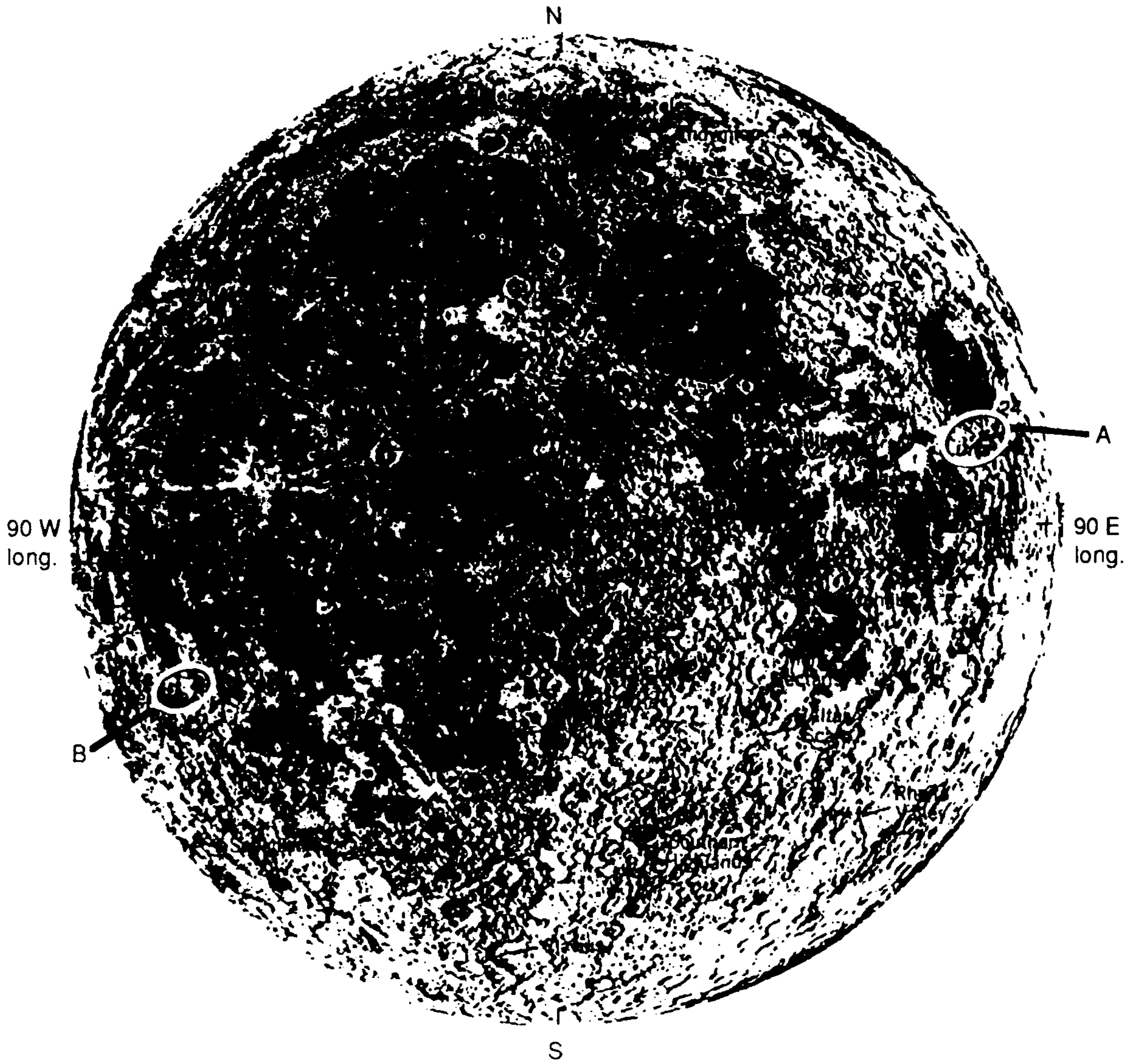

Figure 13. Map of near side of moon, showing the two regions used by Danjon.

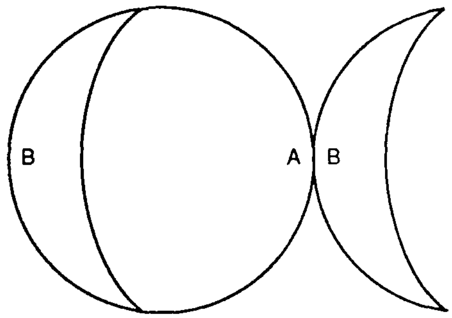

Juxtaposition of two images

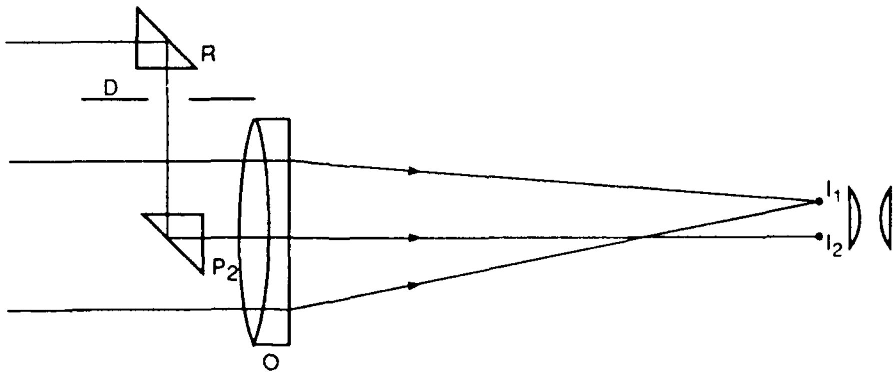

Figure 14. Schematic diagram of the cat's-eye photometer (from Reference [3]).

However, this ratio is also given in terms of the earth's reflectance properties as

$$\frac{I_E}{I_S} = \frac{1}{R_{EM}^2}\frac{d\sigma_E}{d\Omega}(\phi) = \frac{1}{R_{EM}^2}\,\pi R_E^2\,\frac{1}{\pi}p_E f_E(\phi)\ . \qquad (6-3)$$

where R_{EM} is the earth-moon distance, and p_E and f_E are the earth's geometric albedo and phase function. Upon equating (6-2) and (6-3) and solving for $p_E f_E$, we find

$$p_E f_E(\phi) = \left(\frac{R_{EM}}{R_E}\right)^2 D_{AB} f_M(\psi)\ . \qquad (6-4)$$

Danjon used a separate series of comparisons between the intensities of the moon and the sun to determine f_M, as shown in Figure 15. Using this result, together with his observations of D_{AB}, he could determine $p_E f_E$ (or, equivalently, I_E/I_S) from Equation (6-2), as shown in Figure 16.

Finally, the albedo is given as

$$A = \int_{-\pi}^{\pi} p_E f_E(\phi)\sin(\phi)d\phi\ , \qquad (6-5)$$

which is evaluated numerically after extrapolation to unmeasured phase angles. Separate values for p_E and q can be obtained by an extrapolation to $\phi = 0$.

Danjon's results show a number of interesting features. The daily means of the observations vary more widely than would be expected on the basis of the variation of measurements on a single night; this can be attributed to daily changes in cloud cover. A seasonal variation was also evident (see Figure 17), which is of the same shape as that of the ERBE measurements (Figure 1), but a factor of five larger in amplitude. Observations at several wavelengths also indicated that the earth's color changes with season. (These last two points were confirmed by the observations of Dubois [12].) No secular (annual or longer) variations were found.

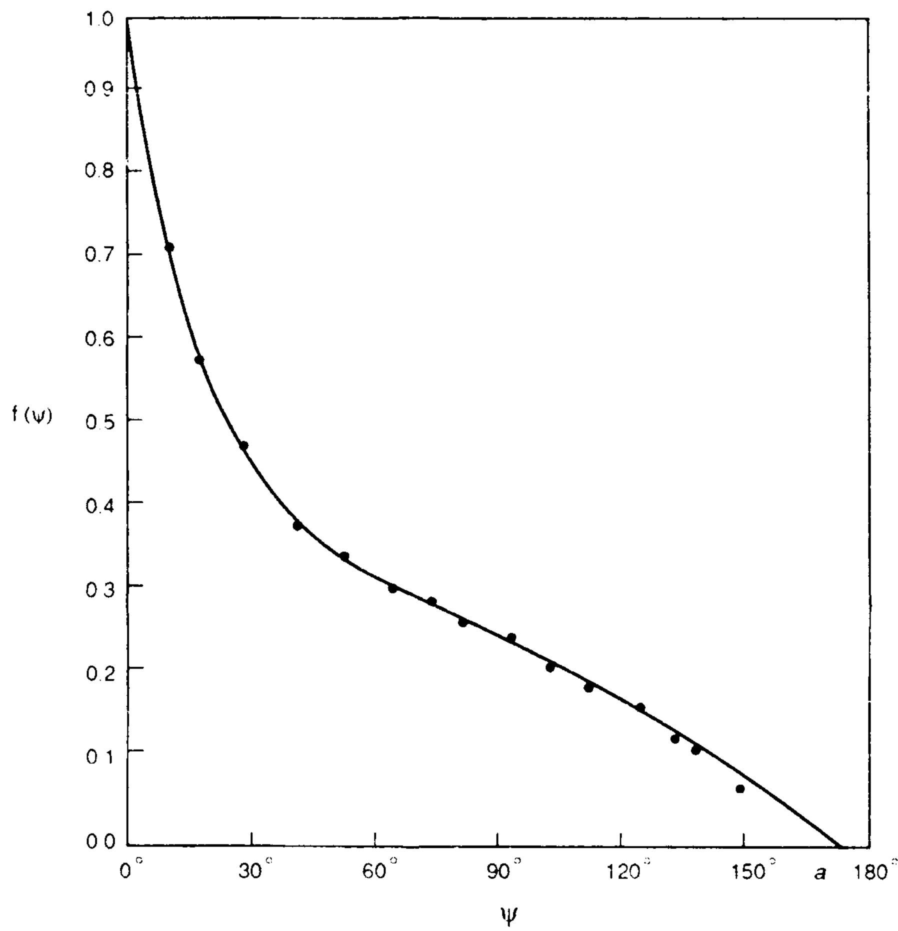

Figure 15. The phase function $f_M(\Psi)$ as determined by Danjon [3].

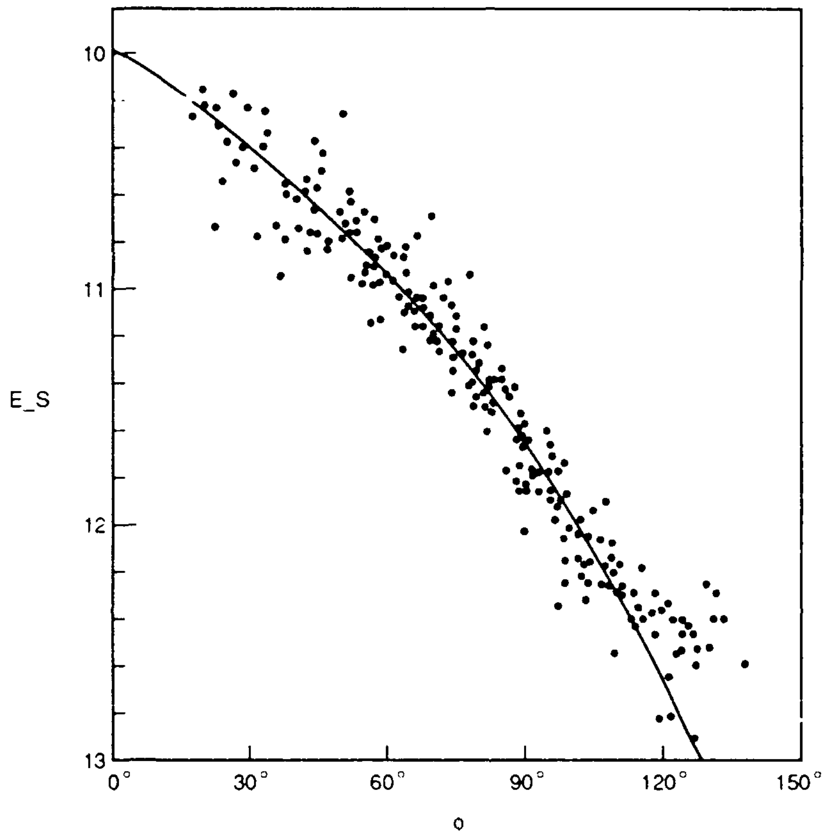

Figure 16. Abscissae, phase angle of the earth; ordinates, magnitude difference (as seen from the moon) between earth and sun. Corrected to mean distances and for seasonal variations (from Reference [3]).

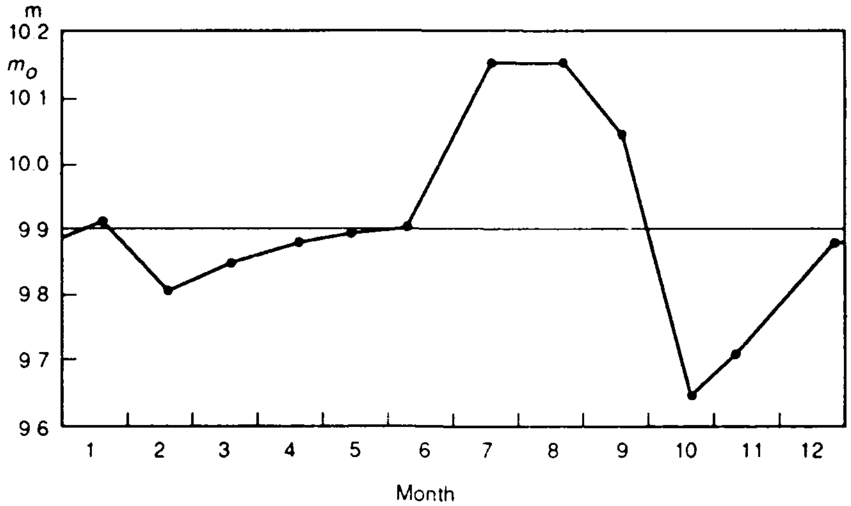

Figure 17. Variation of the monthly mean intensity of earthshine, expressed in magnitudes (from Reference [3])

In order to obtain the Bond albedo, Danjon's measurements in the visual must be corrected for the balance of the shortwave radiation (half of the sun's intensity is a wavelength greater than 0.7 μm). Estimates of this correction were made by Fritz [13], who also took into account that the Western Hemisphere most frequently observed by Danjon has a greater fraction of land than the globe as a whole. As the earth's albedo decreases with increasing wavelength (after all, the earth is sometimes called the "blue planet"), Fritz finds that Danjon's visual albedo of 0.40 corresponds to a Bond albedo of 0.36.

A second correction to the earthshine measurements must be made for the "opposition effect" present in the lunar reflectance properties; to our knowledge, this has not been considered previously. Observations of the moon [14, 15] (see Figure 18) show that the moon's phase function can rise by as much as a factor of 2 as $|\psi|$ decreases from 5 degrees to 0 (exact *backscattering). This enhancement* is caused by the porous nature of the lunar surface [11], and was unknown at Danjon's time since measurements close to $\psi = 0$ are hindered by lunar eclipses. (Note that the smallest angle measured in Danjon's lunar phase curve is only 11 degrees.) The extent of the small-angle rise varies over different regions of the lunar surface [14 15], but can easily be the 20 percent required to reduce Fritz's 0.36 to 0.29. This latter value is consistent with the ERBE satellite estimates of 0.30 [6].

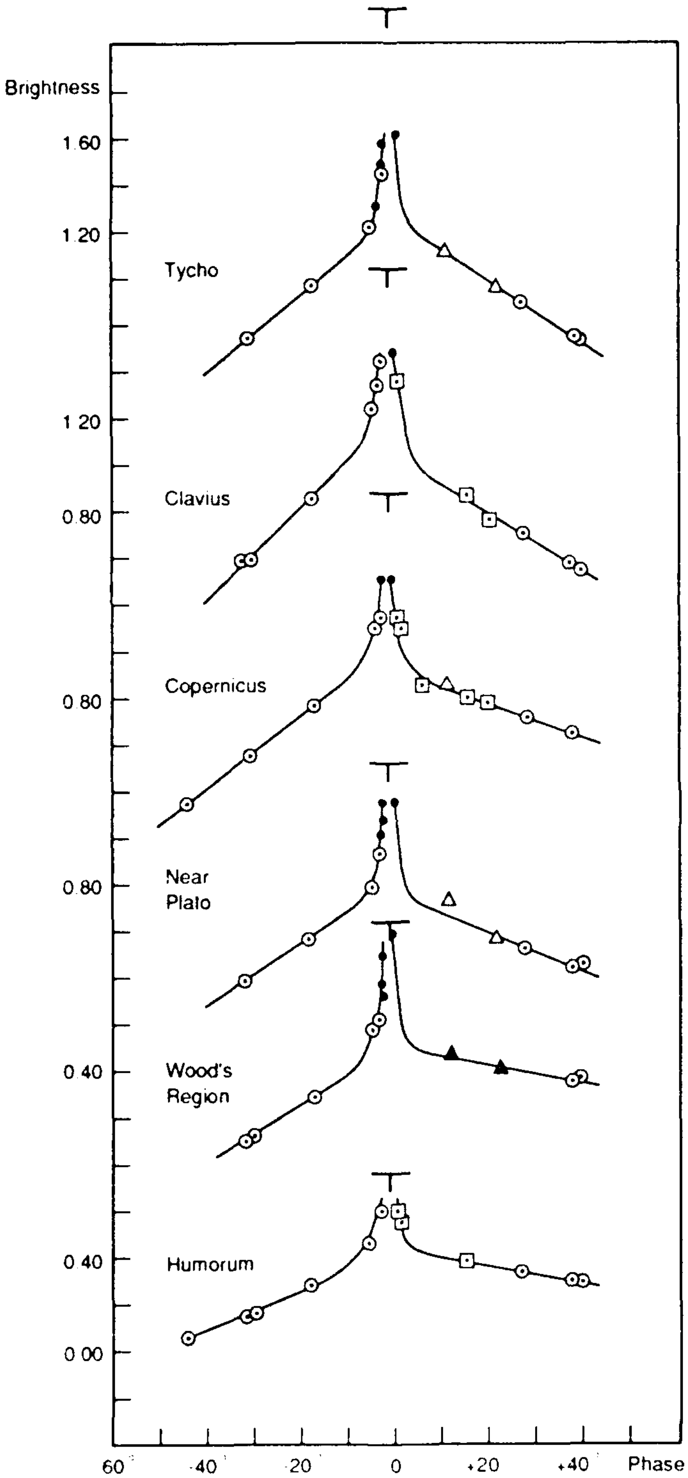

Figure 18. Brightness observed for various features on the moon as a function of phase. The T symbols include the extrapolation to zero phase (from Reference [13])

7 THE POTENTIAL FOR MODERN MEASUREMENTS

In the modern context, earthshine measurements have a number of attractive aspects. Ground-based measurements that integrate on a global scale are rare and the albedo is a basic parameter of the climate system. Earthshine measurements would complement more detailed satellite studies and could serve, at a minimum, as a cross check on the scene models used. That is, given meteorological data, these models make clear, non-trivial predictions of the time variation of the earthshine, which should be checked observationally.

Modern photometry can do significantly better than the state of the art in the 1920s. CCDs with 1024 × 1024 resolution and sufficient dynamic range to observe both the sunshine and the earthshine simultaneously can be purchased off the shelf. This would supplant Danjon's two-spot scheme. Together with a small (say 8") reflecting telescope, the total cost should be under \$50,000. Two-dimensional imaging arrays that could extend observations to the near IR are also available, although at a somewhat greater cost. It might also be possible to illuminate the moon directly with a ground-based laser to measure the lunar geometric albedo. This latter is essential to deterring the absolute value of the earth's albedo but is unimportant if only changes are of interest.

Beyond a set of demonstration measurements, a long term monitoring program could make unique contributions to global change studies. Three observation sites spaced around the globe are sufficient for continuous coverage during the majority of the month when the earthshine is intense enough to be observed. Interannual variations of the albedo are clearly of great interest, as are their correlations to global mean surface temperature. (As interannual temperature variations are ≤ 0.5K, we might expect albedo variations $\lesssim 0.005$.) The phase function itself may be more sensitive to global warming than is the phase integral; this can, of course, be studied with models.

Today almost all GCMs give geographic models of surface albedos. Various parameterization schemes are used to capture changes in ice and snow cover, alteration of vegetation, etc. One of the results of running a GCM is the albedo determined as the difference between incoming solar radiation and the calculated outgoing infrared radiation. In this calculation the effects of assumptions about the surface and cloudiness are integrated over the globe. A measurement of the integrated albedo, such as that obtained from observations of earthshine, would provide a valuable check as to how well the model was representing the surface and cloud components of the albedo. A comparison of the seasonal variation in observed and computed albedo would provide another check on GCMs. If the observation could be maintained over a long interval, then the secular changes in observed and computed albedo could be compared.

Finally, there is the interesting possibility of an historical record of earthshine measurements spanning the 60 years since Danjon's work. Our preliminary investigations have turned up only the work of Dubois extending to 1958 [12]. However, if other data exist, they could provide a unique window on the secular change of the earth's climate. [We have recently learned of efforts at the University of Arizona (D. Huffman, private communication) aimed at duplicating Danjon's instrument and observing technique.]

REFERENCES

1. F.W. Very, *Astronomische Nachrichten*, **196**, 269 (1912); *ibid*, **201**, 353 (1915).

2. A. Danjon, *Ann. Obs. Strasbourg*, **2**, 165 (1936).

3. A. Danjon in *The Earth as a Planet*, ed. G. Kuiper (Univ. of Chicago Press, Chicago, 1954), p. 726.

4. F.A. Franklin, *J. Geophys. Res.*, **72**, 2963 (1967).

5. M.C. MacCracken and F.M Luther, eds., "*Detecting the Climatic Effects of Increasing Carbon Dioxide*," Report DOE/ER-0235 (1985).

6. G.G. Gibson et al., *SPIE*, **1299**, 253 (1990).

7. R. Chervin, private communication.

8. R. Kandel, *Beitr. Phys. Atmosph.*, **56**, 322 (1983).

9. B. Lyot and A. Dollfus, *C.R. Acad. Sci., Paris*, **228**, 1773 (1949).

10. M. Rougier, *Ann. Obs. Strasbourg*, **2**, Part 3, 203 (1933).

11. B. Hapke, in "*Physics and Astronomy of the Moon*," *2nd edition*, ed. Z. Kopal (Academic Press, New York, 1971), p. 155.

12. J. E. Dubois, Ciel et Terre **59**, 375 (1943); Bull. Astrom. **13**, 193 (1974); Proces-Verbaux de la Societe de Sciences Physiques et Naturelles de Bordeaux, 24 avril 1958, 1.

13. S. Fritz, *J. Meteor.*, **6**, 277 (1949).

14. T. Gehrels, D. Coffeen, and T. Owings, *Astron. J.*, **69**, 826 (1964).

15. J. van Diggelen, *Planet. Space. Sci.*, **13**, 271 (1965).

16. R.L. Wildey, *Science*, **200**, 1265 (1978).

DISTRIBUTION LIST

Thomas Ackerman
Pennsylvania State University
Dept of Meteorology
503 Walker Building
University Park, FA 16802

Dr Ralph W Alewine
Director/NMRO
DARPA
3701 North Fairfax Drive
Arlington, VA 22203

Dr James Anderson
Department of Chemistry
Harvard University
ESL
40 Oxford Street
Cambridge, MA 02138

Mr John M Bachkosky
Deputy DDR&E
The Pentagon
Room 3E114
Washington, DC 20301

Dr Dave Bader
Pacific N W Laboratory
PO Box 999
Battelee Blvd
Richland, WA 99352

Dr Joseph Ball
Central Intelligence Agency
Washington, DC 20505

Dr Bruce R Barkstrom
NASA Langley Research Center
MS 420
Hampton, VA 23665-5225

Dr Timothy P Barnett
Climate Research Group
Scripps Institution of Oceanography
A-024
UCSD
La Jolla, CA 92093

Sumner Barr
Los Alamos National Laboratory
Mail Stop K305
Los Alamos, NM 87545-0000

Don Beran
WPL/ERL/NOAA
Mail Code: R/E/WP
325 Broadway
Boulder, CO 80303

Dr Kenneth Bergman
Earth Science Support Office
NASA Headquarters
Suite 230
600 Maryland Avenue SW
Washington, DC 20024

Dr Arthur E Bisson
DASWD(OASN/RD&A)
The Pentagon
Room 5C675
Washington, DC 20350-1000

DISTRIBUTION LIST

Dr Donna Blake
Division of Atmospheric Sciences
National Science Foundation
1800 G Street
Washington, DC 20550

Dr Barry Boehm
Director/SSTO
DARPA
3701 North Fairfax Drive
Arlington, VA 22203-1714

Dr. Albert Brandenstein
Chief Scientist
Office of Natl Drug Control Policy
Executive Office of the President
Washington, DC 20500

Dr Francis Bretherton
SSEC
University of Wisconsin
1225 W Dayton Street
Madison, WI 53706

Mr. Edward Brown
Assistant Director/NMRO
DARPA
3701 North Fairfax Drive
Arlington, VA 22203

Dr. Herbert L Buchanan, III
Director/DSO
DARPA
3701 North Fairfax Drive
Arlington, VA 22203

Dr. Curtis G. Callan, Jr.
Physics Department
Princeton University
P.O. Box 708
Princeton NJ 08544

Peter Campbell
Argonne National Laboratory
9700 South Cass Avenue
Argonne, IL 60439

Dr Fenton Carey
Atmos & Climate Research
Office of Energy Research
Department of Energy
MS ER-76
Washington, DC 20585

Dr Robert Cess
Institute for Terr and Planet Atmos
State University of New York
Stoney Brook, NY 11794-2300

Dr Moustafa T Chahine
Chief Scientist
Jet Propulsion Laboratory
MS 180-904
4800 Oak Grove Drive
Pasadena, CA 91109

Dr Robert Chervin
National Center for Atmospheric Research
P O Box 3000
Boulder, CO 80703-3000

DISTRIBUTION LIST

Chief, Library Branch
AD-234.2, FORS
US Department of Energy
Washington, DC 20585

Brig Gen Stephen P. Condon
Deputy Assistant Secretary
Management Policy & Program Integration
The Pentagon, Room 4E969
Washington, DC 20330-1000

Dr. Wendell A. Childs
Teledyne Brown Engineering
P.O. Box 070007
300 Sparkman Drive NW
Huntsville, AL 35807-7007

Ambassador Henry F. Cooper
Director/SDIO-D
The Pentagon, Room 1E1081
Washington, DC 20301-7100

Dr. Ferdinand N. Cirillo, Jr.
Central Intelligence Agency
Washington, DC 20505

Dr Robert W Corell
Assistant Director of Geo Sciences
National Science Foundation
Room 510
1800 G Street NW
Washington, DC 20550

Steve Clifford
NOAA, Wave Propagation Laboratory
325 Broadway
R/E/WP5
Boulder, CO 80303-3328

Ted S Cress
Pacific Northwest Laboratory
PO Box 999, K1-74
Battelle Boulevard
Richland, WA 99352

Cmdr & Program Executive Officer
US Army/CSSD-ZA
Strategic Defense Command
PO Box 15280
Arlington, VA 22215-0150

D T I C (2)
Defense Technical Information Center
Cameron Station
Alexandria, VA 22314

Dr James Cogan
USA Atmospheric Sciences Lab
ATTN: SLCAS-BW-W
White Sands Missile Range
Los Cruzes, NM 88002-5501

Darpa Library
3701 North Fairfax Drive
Arlington, VA 22203

DISTRIBUTION LIST

Mr. John Darrah
Senior Scientist and Technical Advisor
HQAF SPACOM/CN
Peterson AFB, CO 80914-5001

Dr. Gary L. Denman
Director
DARPA/DIRO
3701 North Fairfax Drive
Arlington, VA 22203-1714

Marv Dickerson
Lawrence Livermore National Lab
PO Box 808, L-262
7000 E Avenue
Livermore, CA 94550

Director, Ames Laboratory (2)
Iowa State University
Ames, Iowa 50011

Col Doc Dougherty
DARPA/DIRO
3701 North Fairfax Drive
Arlington, VA 22203-1714

Robert Ellingson
University of Maryland
Department of Meteorology
2213 Space Sciences Building
College Park, MD 20742

Mr. John Entzminger
Chief, Advance Technology
DARPA/DIRO
3701 North Fairfax Drive
Arlington, VA 22203

Capt Kirk Evans
Director Undersea Warfare
Space & Naval Warfare System
Command
Department of the Navy
Washington, DC 20363-5100

Dr Jay Fein
Div of Atmospheric Sciences
National Science Foundation
Room 644 NSF
1800 G Street NW
Washington, DC 20550

Dr Jack Fellows
Science and Space Program
Office of Management & Budget
Room 8001
725 17th Street NW
Washington, DC 20503

Dr. Stanley M. Flatte'
678 Spring Street
Santa Cruz, CA 95060

Mr. F. Don Freeburn (25)
US Department of Energy, Code ER-33
Mail Stop G-236
Washington, DC 20585

DISTRIBUTION LIST

Dr Edward A Frieman
Director
Scripps Institution of Oceanography
Directors Office 0210
9500 Gilman Drive
La Jolla, CA 92093-0210

Dr D D Grantham
Geophysics Directorate
Phillips Laboratory
AF Systems Command
Hanscom AFB, MA 01731-5000

Dr. Dave Galas
Associate Director for
Health & Environmental Research
ER-70/GTN
US Department of Energy
Washington, DC 20585

Jeff Griffin
Pacific Northwest Laboratory
PO Box 999, MS K5-10
Battelle Boulevard
Richland, WA 99352

Dr Catherine Gautier
Mission Research Corporation
P O Drawer 719
Santa Barbara, CA 93102-0719

Ronald Hadlock
Pacific Northwest Laboratory
PO Box 999, K6-03
Battelle Boulevard
Richland, WA 99352

Dr. Lance Glasser
DARPA/ESTO
3701 North Fairfax Drive
Arlington, VA 22203-1714

Dr J Michael Hall
US Department of Commerce
Director/Office of Climate &
Atmospheric Research/NOAA R/CAR
1335 East/West Highway
Silver Springs, MD 20910

Dr A Goroch
Naval Oceanographic &
Atmospheric Research Laboratory
Monterey, CA 93943-5006

Mr. Thomas H. Handel
Office of Naval Intelligence
The Pentagon, Room 5D660
Washington DC 20350-2000

Dr. S. William Gouse
Sr. Vice President & General Manager
The MITRE Corporation
Mail Stop Z605
7525 Colshire Dr.
McLean, VA 22102

Dr James Hansen
Goddard Institute for Space
Studies/NASA
2880 Broadway
New York, NY 10025

DISTRIBUTION LIST

Maj Gen Donald G. Hard
Director of Space & SDI Programs
Code SAF/AQS
The Pentagon
Washington, DC 20330-1000

Dr. Robert G. Henderson
Director, JASON Program Office
The MITRE Corporation, MS Z561
7525 Colshire Drive
McLean, VA 22102

Dr. Barry Horowitz
President and Chief Executive Officer
The MITRE Corporation
202 Burlington Road
Bedford, MA 01730-1420

Dr. William E. Howard (2)
Director for Space & Strategic Technology
Office/Assist Secretary of the Army
The Pentagon, Room 3E474
Washington, DC 20310-0103

Dr. Gerald J. Iafrate
US Army Research Office
P.O. Box 12211
4300 South Miami Blvd
Research Triangle Park NC 27709

J A S O N Library (5)
The MITRE Corporation, MS W002
7525 Colshire Drive
McLean, VA 22102

Dr. George Jordy (2)
Director for Program Analysis
US Department of Energy
ER30
OER
Washington, DC 20585

Dr. O' Dean Judd
Los Alamos National Lab
Mail Stop A-110
Los Alamos, NM 87545

Paul Kanciruk
Oak Ridge National Laboratory
One Bethal Valley Road
Oak Ridge, TN 37831-6335

Dr. Steven E. Koonin
Kellogg Radiation Laboratory, 106-38
California Institute of Technology
Pasadena, CA 91125

Mr. Paul Kozemchak
Strategy & Planning
DARPA/DIRO
The Pentagon, Room 4B926
Washington, DC 22003

Dr Chuck Leith
Lawrence Livermore National Laboratory
L-16
PO Box 808
Livermore, CA 94550

DISTRIBUTION LIST

Dr Jean- Francois Louis
Atmospheric and Environmental Research, Inc.
840 Memorial Drive
Cambridge, MA 02139

Dr Peter Lunn
Atmos & Clim Research Division
Office of Energy Research
Department of Energy
MS ER-76
Washington, DC 20585

Dr. Michael Mac Cracken
Atmospheric & Geophysical Science Div
Lawrence Livermore National Lab
P.O. Box 808
L-262
Livermore, CA 24550

Dr Paul Mac Cready
Aerovironment Inc
222 E Huntington Drive
Monrovia, CA 91016

Dr. Gordon J. Mac Donald
Institute on Global Conflict & Cooperation
UCSD/0518
9500 Gilman Drive
La Jolla, CA 92093-0518

Mr. Robert Madden (2)
Department of Defense
National Security Agency
Attn R-9
Ft. George G. Meade MD 20755-6000

Dr Jerry Mahlman
NOAA
Forrestal Campus of Princeton U
G7DL
Princeton, NJ 08542

Dr Robert Malone
Group EES-S
Los Alamos National Lab
MS F 665
Los Alamos, NM 87545

Dr. Arthur F. Manfredi, Jr. (10)
OSWR
Central Intelligence Agency
Washington, DC 20505

Mr. Joe Martin
Director
OUSD(A)/TWP/NW&M
The Pentagon, Room 3D1048
Washington, DC 20301

Robert Mc Intosh
University of Massachusetts
Dept of Elec. and Comp. Eng
Amherst MA 01003

Ron Melton
Pacific Northwest Laboratory
PO Box 999, MS K7-28
Richland, WA 99352

DISTRIBUTION LIST

Paul Michael
Brookhaven National Laboratory
Building 318
Upton, NY 11973

Dr Berrien Moore, III
Director
Institute for the Study of Earth
Ocean & Space
Science & Engineering Research Bldg
Durham, NH 03824-3525

Mr. Ronald Murphy
DARPA/ASTO
3701 North Fairfax Drive
Arlington, VA 22203-1714

Dr. Julian C. Nall
Institute for Defense Analyses
1801 North Beauregard Street
Alexandria, VA 22311

Dr. Gordon C. Oehler
Central Intelligence Agency
Washington, DC 20505

Mr David D Otten
Sr Executive Global Change Initiative
TRW Inc
One Space Park
Building R11 Room 2826
Redondo Beach, CA 90278

Dr. Peter G. Pappas
Chief Scientist
US Army Strategic Defense Command
P.O. Box 15280
Arlington, VA 22215-0280

Dr. Aristedes Patrinos (20)
Director of Atmospheric & Climate Research
ER-74/GTN
US Department of Energy
Washington, DC 20585

Dr. Bruce Pierce
USD(A)/DS
The Pentagon, Room 3D136
Washington, DC 20301-3090

Dr. Arati Prabhakar
DARPA/MTO
3701 North Fairfax Drive
Arlington, VA 22203-1714

Dr Veerabnadran Ramanathan
California Space Institute
Scripps Institution of Oceanography
University of California San Diego
Mail Code A-021
La Jolla, CA 92093-0221

David Randall
Colorado State University
Department of Atmospheric Science
Ft Collins, CO 80523

DISTRIBUTION LIST

Mr. John Rausch (2)
Division Head 06 Department
DAVOPINTCEN
4301 Suitland Road
Washington, DC 20390

Records Resources
The MITRE Corporation, MS W115
7525 Colshire Drive
McLean VA 22102

Dave Renne
Battelle Washington Office
370 L'Enfant Promenade, SW
Suite 900
Washington, DC 20024-2115

Research Librarian (2)
Brookhaven National Laboratory
Upton, NY 11973

Dr. James J. Richardson
Assistant Director/LSO
DARPA
3701 North Fairfax Drive
Arlington, VA 22203-1714

Dr. Fred E. Saalfeld
Director, Office of Naval Research
800 North Quincy Street
Arlington, VA 22217-5000

Ken Sassen
University of Utah
Department of Meterology
819 William Browning Building
Salt Lake City, UT 84112

Mr. John Schuster
Technical Director of Submarine
and SSBN Security Program
Department of the Navy OP-02T
The Pentagon, Room 4D534
Washington, DC 20350-2000

Steven Schwartz
Brookhaven National Laboratory
Applied Sciences Division
51 Bell Avenue. Building 426
Upton, NY 11973

Dr. Barbara Seiders
Chief of Research
Office of Chief Science Advisor
Arms Control & Disarmament Agency
Washington, DC 20451

Dr. Philip A. Selwyn
Director, Office of Naval Technology
Room 907
800 North Quincy Street
Arlington, VA 22217-5000

Dr Albert Semtner
Department of Oceanography
Naval Post Grad School
Code 68
Monterey, CA 93949

DISTRIBUTION LIST

Paul Singley
Oak Ridge National Laboratory
PO Box 2008
Building 4500N, MS 6207
Oak Ridge, TN 37831-6207

Dr. A. T. Stair
Stewart Radiance Laboratory
139 The Great Road
Bedford, MA 01730

Douglas L Sisterson
Argonne National Laboratory
ER-203
9700 S. Cass Avenue
Argonne, IL 60439

Dr Allan Steed
Space Dynamics Laboratory
Utah State University
Logan, UT 84322-4140

Prof. William Smith
Director of CIMSS
University of Wisconsin
Madison WI 53706

Dr Graene L Stephens
Dept of Atmospheric Sciences
Colorado State University
Ft Collins, CO 80523

Prof Richard C J Somerville
Scripps Institution of Oceanography
UCSD
Mail Code 0224
8605 La Jolla Shores Drive
La Jolla, CA 92093-0224

Gerald Stokes
Pacific Northwest Laboratory
Battelle Boulevard, MS K1-74
Richland, WA 99352

Dr. David Sowle
Mission Research Corporation
PO Drawer 719
Santa Barbara, CA 93102-0719

Mr. Charles E. Stuart
UWO
DARPA
3701 North Fairfax Drive
Arlington, VA 22203-1714

Dr. Stephen L. Squires
Director/CSTO
DARPA
3701 North Fairfax Drive
Arlington, VA 22203-1714

Superintendent
Code 1424
ATTN: Documents Librarian
Naval Postgraduate School
Monterey, CA 93943

DISTRIBUTION LIST

M. Tom Swartz
Actg Dir/SPO
DARPA
3701 North Fairfax Drive
Arlington, VA 22203-1714

Dr. C. Bruce Tarter
LLNL
PO Box 808
L-295
Livermore, CA 94550

Technical Information Center (2)
US Department of Energy
PO Box 62
Oak Ridge, TN 37830

Technical Librarian (2)
Argonne National Laboratory
9700 South Cass Avenue
Chicago, IL 60439

Technical Librarian (2)
Los Alamos National Laboratory
PO Box 1663
Los Alamos, NM 87545

Technical Librarian (2)
Oak Ridge National Laboratory
Box X
Oak Ridge, TN 37831

Technical Librarian (2)
Pacific Northwest Laboratory
Battelle Boulevard
PO Box 999
Richland, WA 99352

Technical Librarian (2)
Sandia National Laboratory
PO Box 969
Livermore CA 94550

Technical Librarian (2)
Lawrence Livermore National Laboratory
PO Box 808
Livermore CA 94550

Technical Librarian (2)
Sandia National Laboratories
PO Box 5800
Albuquerque, NM 87185

Technical Librarian (2)
Lawrence Berkeley Laboratory
One Cyclotron Road
Berkeley, CA 94720

Colonel Jack Thorpe
DARPA/DIRO
3701 North Fairfax Drive
Arlington, VA 22203-1714

DISTRIBUTION LIST

Dr Shelby Tilford
NASA Headquarters
Code -SE
600 Independence Avenue SW
Washington, DC 20546

U S Department Of Energy
Procurement and Contracts Division
(DOE IA No. DE-AI05-90ER30174)
Oak Ridge Operations Office
PO Box 2001
Oak Ridge, TN 37831-8757

Dr. George W. Ullrich (3)
Deputy Director
Defense Nuclear Agency
6801 Telegraph Road
Alexandria, VA 22310

Ms Michelle Van Cleave
Asst Dir/National Security Affairs
Office/Science & Technology Policy
New Executive Office Building
17th and Pennsylvania Ave.
Washington, DC 20506

Mr. Richard Vitali
Director of Corporate Laboratory
US Army Laboratory Command
2800 Powder Mill Road
Adelphi, MD 20783-1145

Professor Steven Warren
Department of Atmospheric Sciences
University of Washington
AK-40
Seattle, WA 98195

Dr Warren Washington
Director
Climate and Global Dynamics Division
NCAR
PO Box 3000
Boulder, CO 80307-3000

Marvin L Wesely
Argonne National Laboratory
9700 S. Cass Avenue
Building 203 ER
Argonne, IL 60439-4843

Dr. Edward C. Whitman
Deputy Assist Secretary of the Navy
C3I Electronic Warfare & Space
Department of the Navy
The Pentagon, Room 4D745
Washington, DC 20350-5000

Dr Bruce Wielicki
NASA Langley Research Center
MS 420
Hampton, VA 23665-5225

W Stanley Wilson
Assistant Administrator
NOAA/NOS
1825 Connecticut Ave. NW, Suite 611
Washington, DC 20235

Col Simon P Worden
National Space Council
Executive Office of the President
Room 423
Washington, DC 20500

DISTRIBUTION LIST

Mr. Donald J. Yockey
Under Secretary of Defense for
Acquisition
The Pentagon, Room 3E933
Washington, DC 20301

Bernie Zak
Sandia National Laboratory
PO Box 5800, Division 6321
Albuquerque, NM 87185

Dr. Linda Zall
Central Intelligence Agency
Washington, DC 20505